

Significant Upregulation of Alzheimer's β -Amyloid Levels in a Living System Induced by Extracellular Elastin Polypeptides

Chao Ma⁺, Juanjuan Su⁺, Yao Sun⁺, Yang Feng, Nolan Shen, Bo Li, Yingxia Liang, Xintong Yang, Hui Wu, Hongjie Zhang, Andreas Herrmann,* Rudolph E. Tanzi, Kai Liu,* and Can Zhang*

Abstract: Alzheimer's disease (AD) is a neurodegenerative disorder and the primary cause of age-related dementia. The etiology of AD is complex and has not been completely elucidated. Herein, we report that treatment with elastin-like polypeptides (ELPs), a component of the brain extracellular matrix (ECM), significantly increased the levels of AD-related amyloid- β peptides ($A\beta$) both *in vitro* and *in vivo*. Regarding the molecular mechanism(s), the upregulation of $A\beta$ levels was related to increased proteolytic processing of the amyloid precursor protein. Furthermore, nesting tests demonstrated that the ELP-treated animals showed significant neurobehavioral deficits with cognitive impairment. These results suggest that the elastin is associated with AD-related pathological and behavioral changes. This finding presents a new aspect for Alzheimer's amyloidosis event and provides a great promise in developing ELP-based model systems to better understand the pathogenesis of AD.

Introduction

Alzheimer's disease (AD) is a progressive neurodegenerative disorder and the major cause of dementia in the elderly. Considerable evidence shows that upregulation and accumulation of a small peptide, called amyloid- β ($A\beta$), are primary pathogenic events of AD,^[1–3] which drive the other critical components involved in AD pathologies, including tau protein hyperphosphorylation and neuroinflammation.^[4–9]

The etiology of AD is complex and the mechanistic elucidation of AD pathogenesis remains inconclusive. It has been challenging to comprehensively determine pathological events contributing to the onset and progression of AD.^[10,11] Presently, there is an urgent need to identify and investigate new factors that may trigger $A\beta$ overproduction in the neuronal microenvironment and to further unravel the pathogenesis of AD.

The extracellular matrix (ECM) plays an important role in regulating the development and homeostasis of cells in the central nervous system as well as other parts of human body and several therapies targeting ECM are actively being developed.^[12,13] Concomitantly, the role of ECM in neuropathology has also been of growing interests. The components of ECM in the brain include basement membranes (BM) surrounding cerebral vessels and perineuronal nets (PN), as well as neural interstitial matrix (NIM).^[14] The macromolecules from the PN and NIM, such as tenascin R and proteoglycan, have been studied in the context of neurodegeneration due to their maintenance features.^[14–16] In terms of age-related AD pathology, however, little attention has been paid to the fibrous proteins (for example, elastin) in the BM region. There are reports that elastin can be substantially fragmented and released with aging, yet the effects of these released elastin polypeptides on AD pathogenesis remain elusive.^[17,18]

[*] Dr. C. Ma,^[+] Y. Feng, B. Li, Prof. Dr. H. Zhang, Prof. Dr. K. Liu
 State Key Laboratory of Rare Earth Resource Utilization,
 Changchun Institute of Applied Chemistry,
 Chinese Academy of Sciences, 130022, Changchun (China)
 E-mail: kai.liu@ciac.ac.cn



Dr. C. Ma,^[+] X. Yang, Prof. Dr. A. Herrmann
 Zernike Institute for Advanced Materials
 Nijenborgh 4, 9747 AG Groningen (The Netherlands)


Dr. J. Su,^[+] Y. Feng, N. Shen, Y. Liang, Prof. Dr. R. E. Tanzi,
 Prof. Dr. C. Zhang
 Genetics and Aging Research Unit, McCance Center for Brain Health,
 MassGeneral Institute for Neurodegenerative Disease,
 Department of Neurology,
 Massachusetts General Hospital and Harvard Medical School
 Charlestown, MA (USA)
 E-mail: zhang.can@mgh.harvard.edu

Y. Sun,^[+] Prof. H. Wu
 National Engineering Laboratory for AIDS Vaccine,
 School of Life Sciences, Jilin University, Changchun 130012 (China)

Prof. Dr. A. Herrmann
 DWI—Leibniz Institute for Interactive Materials
 Forckenbeckstr. 50, 52056 Aachen (Germany)
 and
 Institute of Technical and Macromolecular Chemistry,
 RWTH Aachen University
 Worringerweg 2, 52074 Aachen (Germany)
 E-mail: herrmann@dw.rwth-aachen.de

[*] These authors contributed equally to this work.

 Animal experiments are in agreement with the guidelines of the
 Regional Ethics Committee for Animal and Clinical Experiments of
 Jilin University Institutional Animal Care and Use. Supporting
 information and the ORCID identification number(s) for the
 author(s) of this article can be found under:
<https://doi.org/10.1002/anie.201912399>.

 © 2019 The Authors. Published by Wiley-VCH Verlag GmbH & Co. KGaA. This is an open access article under the terms of the Creative Commons Attribution License, which permits use, distribution and reproduction in any medium, provided the original work is properly cited.

Herein, we demonstrate that the elastin-like polypeptides (ELPs) play a previously unrecognized role in A β upregulation. ELPs significantly induced the overproduction of A β peptides in Alzheimer's model cells (7PA2 cells, a Chinese hamster ovary cell line that stably expresses mutant human amyloid precursor protein (APP)), resulting in amounts of A β 5–10 times higher than those in control groups. The behavior of A β overproduction can be further actively tuned by temperature owing to the polymeric properties of ELPs. Furthermore, A β upregulation was detected in the brains of mice at two months post ELP injection. Furthermore, nesting tests demonstrated that the mice showed progressive impairment of cognitive behavior in a dose-dependent manner. Therefore, our finding has revealed that ELPs are novel and important modulators that upregulate Alzheimer's A β proteins, and thus, also provide valuable knowledge to better understand the pathogenesis of AD.

Results and Discussion

The ELPs are a family of genetically encoded biopolymers and contain repeats of canonical sequences derived from native elastin. The primary structure of ELPs consists of repetitive pentapeptide units (VPGVG) $_n$ with low complexity (Figure 1A).^[19–21] ELP30, ELP48, and ELP90 with varied

lengths of polypeptide backbones were used in this study. ELP sequences and motifs dictate their physicochemical properties, for example, they are differentially responsive to external stimuli (Figure 1B).^[20] A thermal-related phase transition behavior, termed lower critical solution temperature (LCST), is a typical property of ELPs in aqueous environment. Soluble forms of ELPs can be triggered to become hydrophobic proteinaceous aggregates upon heating over the transitional point (T_t). The LCST is attributed to collective factors involving abrupt changes of hydrated networks surrounding the backbone as well as reduction of water-accessible surface area of the proteins.^[20] To quantitatively evaluate the transitional behavior, UV absorption tests at 350 nm integrated with thermal treatment were performed using ELP90 solutions (Figure 1C). For the group with a concentration of 400 $\mu\text{g mL}^{-1}$, no insoluble aggregate was observed below 34.5 $^{\circ}\text{C}$ (T_t). When the temperature approached the critical point, a blurry phase appeared immediately, instantly reaching a plateau stage exhibiting a maximum degree of opaqueness. This phase change behavior was dependent on the concentration of ELP90. By reducing the concentration to 200 $\mu\text{g mL}^{-1}$, the T_t shifted to 37 $^{\circ}\text{C}$ and it further increased to approximate 39 $^{\circ}\text{C}$ when the solution was 100 $\mu\text{g mL}^{-1}$.

To investigate the interplay of ELPs and A β in cell lines, we utilized an AD-model cell line termed 7PA2 cells, which

has been previously reported and constitutively express familial AD mutation in the APP gene encoding amyloid- β precursor protein (APP). As a first step, cytotoxicity analysis involving the lactate dehydrogenase assay (LDH) was carried out (Figure 2A). ELP90 showed robust biocompatibility due to its proteinaceous nature and all testing groups exhibited an approximately equal ratio of cell viability ($\geq 99\%$). For the investigation of effects of ELP on A β levels, varied amounts of ELP90 were applied to 7PA2 cell media at 30 $^{\circ}\text{C}$ (Figure 2B) and the A β levels (A β 38, A β 40, and A β 42) were quantitatively evaluated by MesoScale A β analysis.^[1] Analysis demonstrated that A β oligopeptides were significantly overproduced at a concentration as low as 50 $\mu\text{g mL}^{-1}$. By raising ELP concentrations first to 100 $\mu\text{g mL}^{-1}$ and further to 200 $\mu\text{g mL}^{-1}$, A β levels, particularly A β 40 and A β 42, dramatically increased by 10–12 fold over control groups (p values < 0.0001). Next, the LCST behavior of

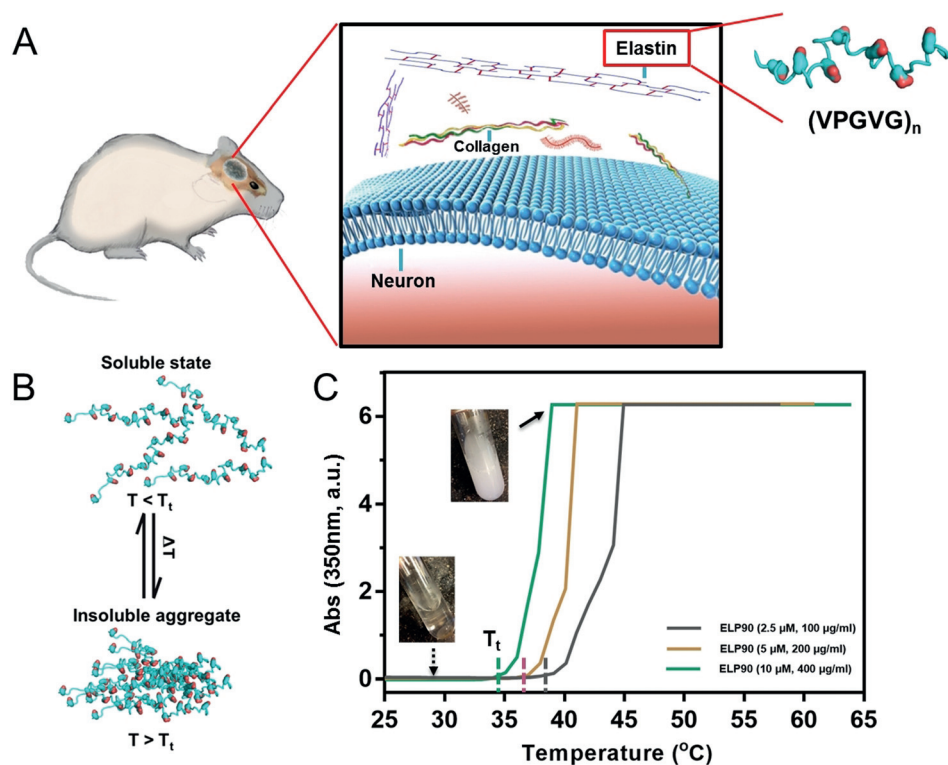


Figure 1. An overview of extracellular elastin. A) A schematic illustration of elastin polypeptides in the brain ECM of a mouse. Elastin is one of the major components in the ECM, consisting of repetitive sequences with low complexity. B) The typical LCST behavior of ELPs. When the temperature is higher than the transitional point ($T > T_t$), soluble elastin polypeptides is triggered to form insoluble aggregates. This process is reversible. C) An investigation of absorption of ELP solution as a function of temperature. The solution stays clear until $T > T_t$. The transition occurs abruptly followed by a plateau with maximum absorption, indicating the blurry phase of the solution.

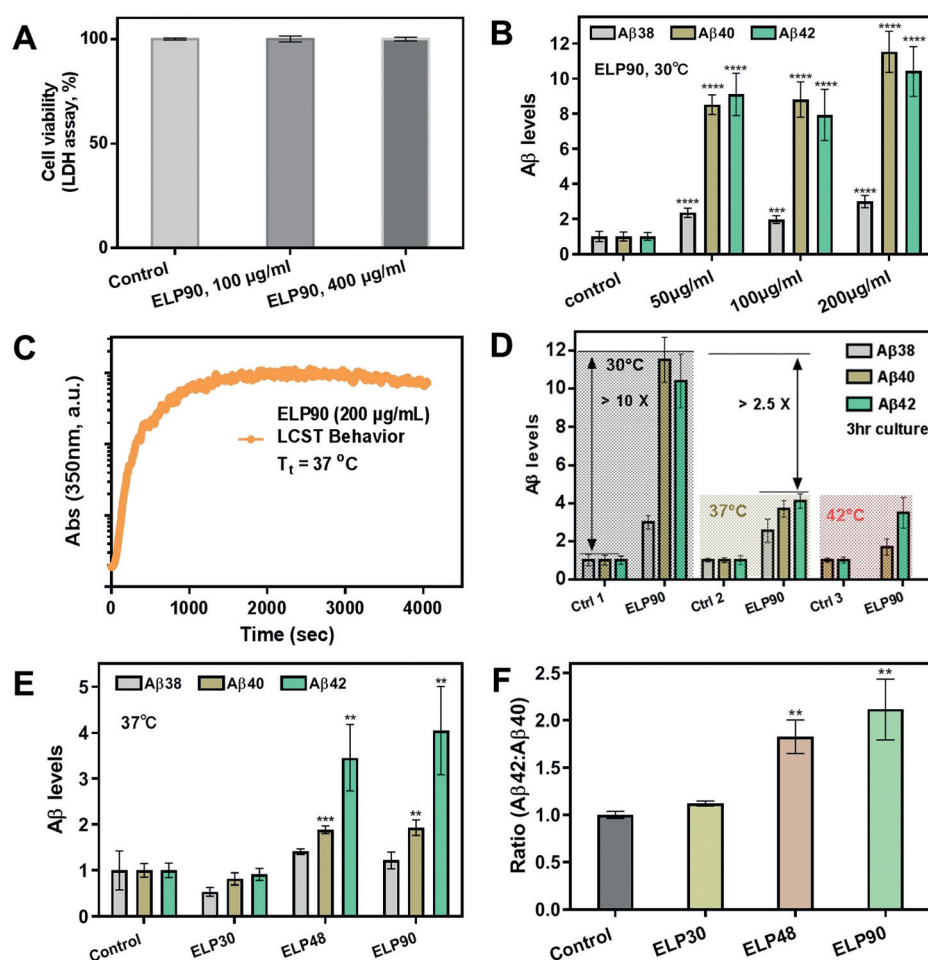


Figure 2. The effects of ELPs on A β peptides in AD 7PA2 cells (a Chinese hamster ovary cell line that stably expresses mutant human amyloid precursor protein (APP)). A) Cytotoxicity tests characterized by the LDH assay. No differences in cell viability were found when comparing ELP-treated cells to the control, indicating excellent biocompatibility of ELPs. B) The changes of A β levels of 7PA2 cells cocultured with ELP90 at 30°C. A β 38, A β 40, and A β 42 showed a significant increase after treatment with ELP90 at a concentration of 50 $\mu\text{g mL}^{-1}$ (p value = 2.05×10^{-5} , 1.66×10^{-8} , and 1.59×10^{-8} , vs. control, respectively), 100 $\mu\text{g mL}^{-1}$ (p value = 1.66×10^{-4} , 4.79×10^{-9} , and 4.26×10^{-7} , vs. control, respectively), and 200 $\mu\text{g mL}^{-1}$ (p value = 3.33×10^{-6} , 4.81×10^{-9} , and 5.57×10^{-8} , vs. control, respectively). C) The LCST profile of ELP90 at 37°C over time. D) Overproduction of A β s can be actively tuned by temperature when treated with ELP. At 30°C, there was a 10-times increase compared with controls (pure cells with PBS). The levels of A β s were 4-fold greater than those of the controls at 37°C and 42°C. E) A β levels can be further tuned by ELPs with varied molecular weight. Levels of A β 40 and A β 42 were significantly increased after treatment with ELP48 (p value = 0.00084 and 0.0045, vs. control, respectively) or with ELP90 (p value = 0.0020 and 0.0056, vs. control, respectively). F) The ratio of A β 42 to A β 40 is dependent on molecular weight of the dosed ELPs. (t-test; mean \pm SD. *, $p < 0.05$; **, $p < 0.01$; ***, $p < 0.001$; ****, $p < 0.0001$).

ELP90 in cell culture was studied at 37°C over time. The absorption changed abruptly in the first 300 s, followed by a long-standing plateau at a maximum value (Figure 2C). Under physiological conditions ($T = 37^\circ\text{C}$) within 3 hours, levels of neurotoxic A β 42 and A β 40 were upregulated 4-fold, although there was an approximately 2.5 times reduction compared with the A β level changes at 30°C. We continued to investigate the interaction of ELP90 and AD cells at 42°C and the data indicate a similar trend as the changes observed at 37°C (Figure 2D). Thus, the effects of ELPs on A β levels are associated with temperature and its aqueous environment.

Thereby, this data demonstrates that the production of A β peptides can be significantly enhanced by ELPs in cell cultures.

Next, ELPs with varied length backbones were used to study A β changes in 7PA2 cells. There was an increasing trend in terms of changes in A β levels when the molecular weights were raised from ELP30 to ELP48 and then to ELP90 (Figure 2E). Specifically, ELP90 showed a 4–5-fold increase of A β 42 in comparison to controls. Notably, the A β 42 to A β 40 ratio (A β 42/A β 40) is related to AD pathology and is a biomarker for AD.^[22,23] The increasing ratio of A β 42/A β 40 in ELP30 groups was almost the same as controls (Figure 2F). Alternatively, a 1.8-fold increase was observed when comparing ELP48 to the control. This value was further enhanced to 2.2 times higher than controls when ELP90 was used ($p < 0.01$). This indicates that larger molecular weights of ELPs are related to higher levels of A β production.

To investigate the underlying mechanism for this observation at a cellular level, multiple biochemical analyses were utilized, including immunofluorescence imaging, western blotting (WB), and quantitative PCR. For the immunofluorescence assay, cells were treated with antibodies G12A (targeting APP C-terminus) and 22C11 (targeting APP N-terminus) and characterized via confocal laser scanning microscopy (Figure 3A–D). The two antibodies specifically recognize full-length APP and isoforms of APP, respectively, and were coupled with secondary antibodies to show different fluorescence. The results showed that there was no significant difference between controls and ELP-treated groups in terms of total APP (Figure 3B,D). At different culturing temperatures (i.e., 30°C and 37°C), no changes in the amounts of APP were observed. Moreover, APP_{ma} and APP_{im}, that is, mature and immature APPs, respectively, were subjected to quantitative WB analysis using the APP8717 antibody and the levels of APP_{ma} and APP_{im} were the same as controls and no significant difference appeared (Figure 3E,F). Collectively, this data implied that the overproduction of A β peptides may not result from

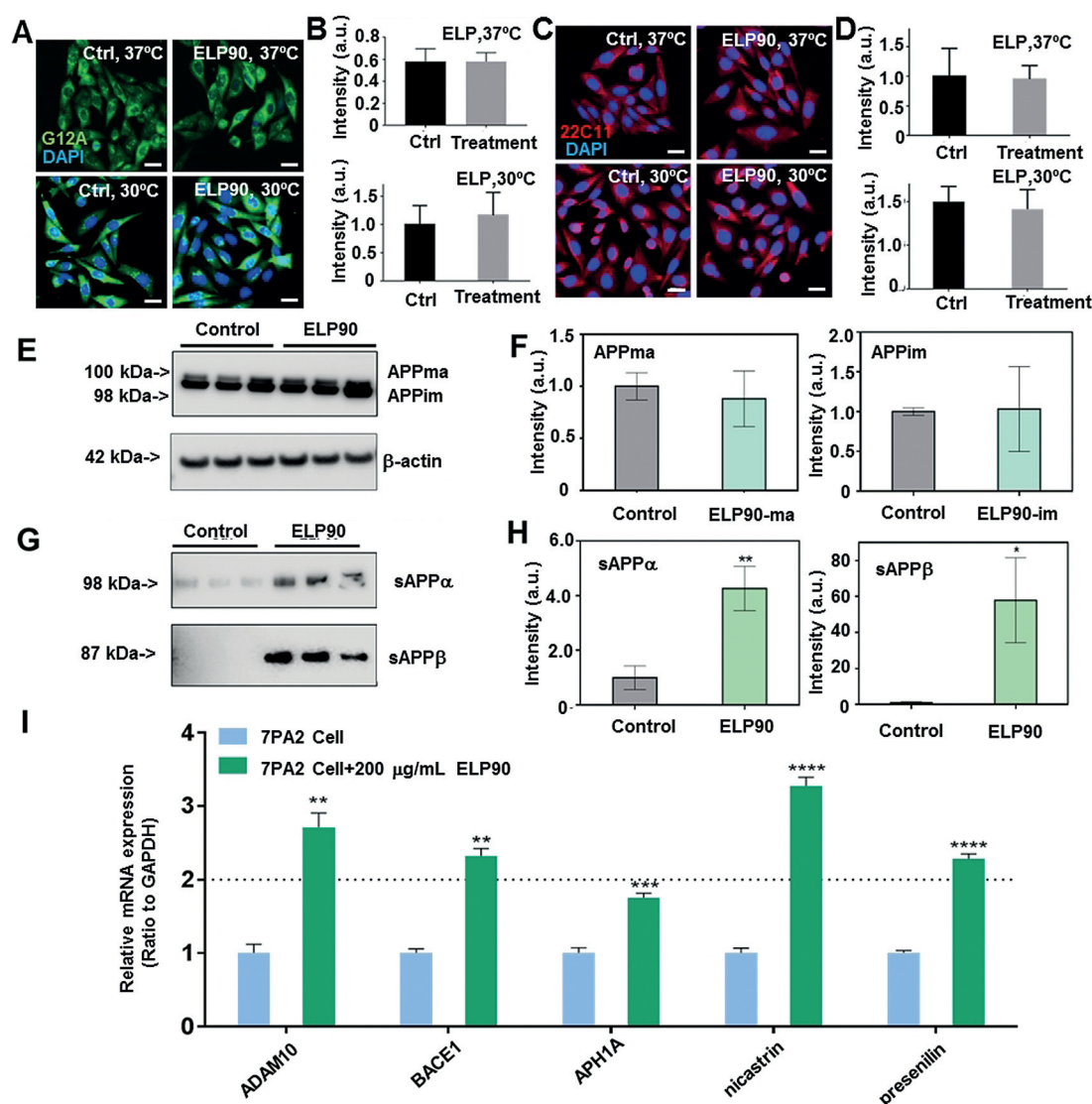


Figure 3. Mechanistic study of upregulation of A β levels. A) The representative fluorescent images for visualization of full-length APPs in 7PA2 cells treated with PBS and ELPs at 30°C and 37°C. The APPs are characterized by G12A antibody and imaged in green. The cell nuclei are stained by DAPI in blue. Scale bar, 20 μ m. B) The quantification of full-length APP levels in cells shown in (A). C) The representative fluorescent images for visualization of isoforms of APP in 7PA2 cells treated with PBS and ELPs at 30°C and 37°C. The APP variants were imaged in red and characterized by 22C11 antibody. Scale bar, 20 μ m. D) Quantification of levels of isoforms of APP presented in (C). E) Western blot (WB) images showing full length APPs, including mature and immature types. The bands were probed with G12A. F) The quantification of APP mature and immature bands. G) The characterization of soluble sAPP α and sAPP β with WB protocol. The control groups were the characterization of PBS-treated cells. H) The quantification of sAPP α and sAPP β . I) The mRNA level changes of α -secretase subunit (ADAM10), β -secretase (BACE1) and γ -secretase subunits (APH1A, nicastrin, and presenilin) after treatment with 200 μ g/ml ELP90 for 24 hours were analyzed by RT-PCR. The 7PA2 cells treated without ELP90 were controls and the mRNA levels are normalized to 1. Data from triplicate tests were collected. (t-test; $n = 3$ per each group); All data are presented as mean \pm S.E.M. *, $p < 0.05$; **, $p < 0.01$; ***, $p < 0.001$; ****, $p < 0.0001$).

changes in total APP profiles. The production of A β s can be also modulated by processing of full-length APP. Typically, APP can be digested by α -secretases, leading to soluble forms of APP α fragments (sAPP α). β - and γ -secretases sequentially cleave APP, resulting in sAPP β and amyloidogenic A β peptides. Thus, we assessed the levels of sAPP α and sAPP β from the perspective of metabolism and processing. Our results indicated that there was a significant upregulation in sAPP α levels detected by the 6E10 antibody when comparing ELP-treated groups to the control ($p < 0.01$, Figure 3H). This

also held true for the sAPP β levels when comparing ELP-treated groups to the control ($p < 0.05$, Figure 3H). To better understand the mechanism involving APP cleavage when dosing with ELP, mRNA levels of the secretases were quantitatively evaluated using real-time PCR (Figure 3I). Specific primers were designed based on the *ADAM10*, *BACE1*, *APH1A*, *nicastrin*, and *presenilin-1* gene sequences in a *Cricetulus griseus* (Chinese hamster) genome library (see Table S3 in the Supporting Information for a full list).^[24] *ADAM10* and *BACE1* are genes encoding α -secretase and

β -secretase, respectively. APOE4, nicastrin, and presenilin-1 are major subunits of the γ -secretase complex, with presenilin-1 (PSEN1) being the catalytic subunit. GAPDH was used for normalization. The result showed that ELP90 treatment at $200 \mu\text{g mL}^{-1}$ was associated with significant upregulation of mRNA levels of the secretases mentioned above in comparison to controls. Particularly, nicastrin, one of the most important structural units of γ -secretase, displayed a remarkable 3.5-fold increase compared to the control ($p < 0.0001$). Thus, it is possibly the overexpression of γ -secretase that leads to substantial cleavage activities and consequently results in overproduction of neurotoxic A β s.

We further investigated the effects of ELP90 on A β levels and neurobehaviors using animal-based studies. 6-week-old male C57BL/6 mice were utilized and treated with PBS (phosphate buffered saline) or different doses of ELP90 ($50 \mu\text{g mL}^{-1}$, $200 \mu\text{g mL}^{-1}$, or $800 \mu\text{g mL}^{-1}$) via intravenous (i.v.) or intracerebroventricular (i.c.v.) injection as described in Figure S3 in the Supporting Information. Nest-building tests have been reported to indicate cognitive changes in mice and are associated with defects in the medial prefrontal cortex and hippocampus.^[25,26] Thus, we performed nest-building tests in mice one and two months post-ELP90 administration. The majority of mice in PBS groups were given a score of 4, indicating good cognition (Figure 4A,B). In contrast, ELP-treated mice showed a dose-dependent decline in both i.v. and i.c.v. subgroups in the first month (Figure 4A). Worsened cognitive performance was observed in the second month (Figure 4B). We further probed protein changes in one brain hemisphere. Using immunohistochemistry staining (IHC) with 4G8 antibody, we revealed upregulated immunoreactive signals in both hippocampal and cortical areas when comparing the ELP group to the control two months post-treatment (Figure 4C). These evidences indicated a deteriorating tendency of cognition pathology in ELP-treated mice over time.

Next, we performed additional biochemical analyses in plasma and the other brain hemisphere (Supporting Information, Figure S4).^[27] Enzyme-linked immunosorbent assay (ELISA) was employed for quantitative analyses of the concentration of A β 42 and A β 40. In plasma, the A β 42 levels increased after both one-month and two-month treatments, especially in i.v. subgroups (Figure 4D and Supporting Information, Figure S5F). Compared with the PBS group, the concentrations of A β 42 in the RAB fraction (aqueous fraction) of the brain homogenate were significantly increased in the first month, especially in the groups treated with i.v. approach (Supporting Information, Figure S5C). These differences were further enlarged after two-months of treatment (Figure 4E). A similar trend was observed in the RIPA fraction (detergent-soluble fraction, Supporting Information, Figure S5A,D), but no statistical differences were detected in the FA fraction comparing ELP-treated groups to the control (insoluble fraction, Figure S5B and S5E). Furthermore, we investigated the levels of sAPP β by WB. The levels of sAPP β appeared to be elevated in the RAB fractions of brain homogenates, comparing ELP-treated groups to PBS-treated groups. We found that the levels of sAPP β in RAB fractions from $50 \mu\text{g mL}^{-1}$ -dosage animals in both i.v.

and i.c.v. groups did not differ compared to the PBS treatment groups after two-months of treatment. In contrast, the levels in the RIPA fractions showed an approximately 10% increase (Figure 4F and Supporting Information, Figure S6). Thereby in total, the amounts of released sAPP β were increased. Notably, the levels of full length (FL) APP showed no differences in either RAB or RIPA fractions during the whole observation period (Figure 4F and Supporting Information, Figure S6). Thus, this animal-based evidence supported those from cell-based investigations, suggesting that ELPs administration results in increasing A β levels.

Upregulation of A β levels may drive other downstream AD-related pathologic events, including tau hyperphosphorylation. We have shown that administration of ELP90 induced a robust increase of A β levels in both cell and animal models. Next, we investigated whether ELP may affect tau protein hyperphosphorylation using IHC and focusing on the hippocampal CA3 region. We showed that the pTau (phosphorylated at Ser396) positive immunostaining signals were increased in both the soma and dendrite of CA3 hippocampal neurons in animals in the second month after ELP treatment compared to the control animals.^[28] This indicated an increase in tau phosphorylation when the mice were treated with ELPs (Supporting Information, Figure S7). Together, these results show that there are multiple lines of molecular pathologic processes in ELP-treated animals, including upregulation of A β levels as well as increases in tau phosphorylation, which collectively affect AD-related pathological and neurobehavioral progression in these animals.

Conclusion

Here, we investigated the interplay of extracellular elastin proteins and Alzheimer's A β peptides both in vitro and in vivo. It is demonstrated that ELPs can significantly upregulate A β proteins. Particularly, exposure to ELPs can lead to robust increases in A β levels up to ten times higher than controls using mechanisms that involve upregulation of APP proteolytic processing. Furthermore, treatment with ELPs in animals results in both AD-related pathological and neurobehavioral changes, including upregulation of A β levels and cognitive impairment. Collectively, our results suggest that the elastin from brain ECM may be a key player in initiating the neurobehavioral defects and pathological changes underlying AD. Our data also strongly suggest that ELPs, and potentially other relevant biomaterials, should be further investigated, which may serve as valuable model systems to better modulate and completely elucidate the pathogenesis of AD.

Acknowledgements

This work was supported by the Scientific Instrument Developing Project of the Chinese Academy of Sciences (Grant No. ZDKYYQ20180001), K. C. Wong Education Foundation (Grant No. GJTD-2018-09), the National Natural Science Foundation of China (Grant No. 21704099, 21877104,

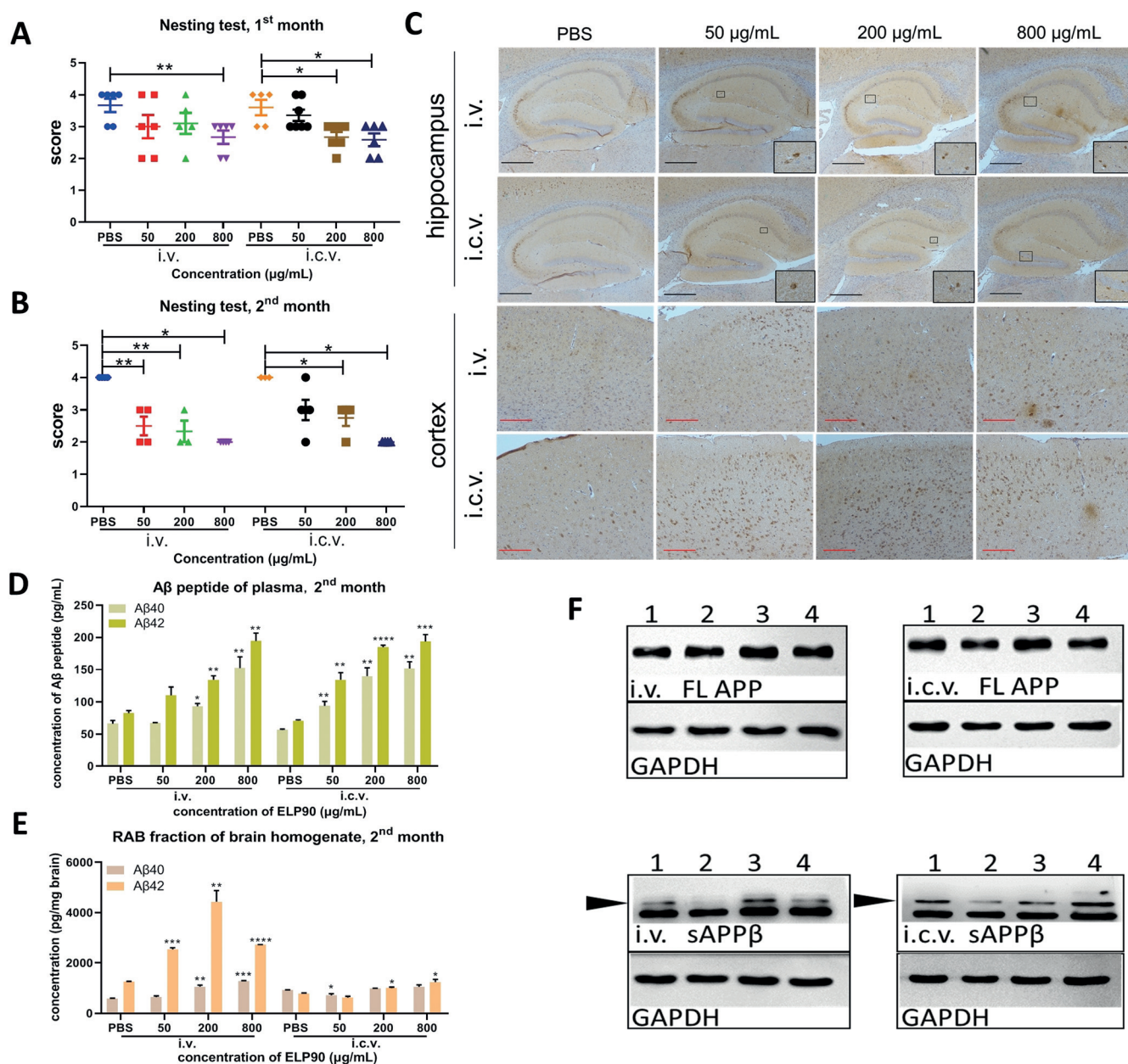


Figure 4. The influence of ELPs on mice. A) Results of nest-building test (NBT) of mice 1 month after treatment. Mice in PBS subgroup show normal cognition (scored 3 to 4) in both i.v. and i.c.v. groups. The scores of ELP-treated mice decline in a dose-dependent fashion in the i.v. group. Particularly, the $800 \mu\text{g mL}^{-1}$ subgroup shows a significant difference compared with controls. A similar tendency occurs in the i.c.v. group, where both $200 \mu\text{g mL}^{-1}$ and $800 \mu\text{g mL}^{-1}$ subgroups show statistically significant differences to controls. $n \geq 5$ for each subgroup. Data are presented as mean \pm S.E.M. $*p < 0.05$, $**p < 0.01$, by Student's t test. B) Results of NBT 2 months after treatment. The scores of PBS subgroups indicate that the mice are in a normal cognitive state. The ELP-treated mice showed worsened behavior. All subgroups in i.v. and i.c.v. groups (except the subgroup of $50 \mu\text{g mL}^{-1}$ in i.c.v.) showed significant differences compared to PBS-treated mice 2 months after treatment. $n \geq 3$ for each subgroup. Data are presented as mean \pm S.E.M. $*p < 0.05$, $**p < 0.01$. C) Detection of A β amyloids in the hippocampus and cortex of mice 2 months after administration of PBS or different concentrations of ELP90. A β ensembles are probed by the 4G8 antibody with IHC assay in the corresponding brain regions. Compared with PBS-treated mice, the ELP-treated mice show a noticeable increase of 4G8 antibody immunoreactive signals in both hippocampus (marked by black frame) and frontal cortex. Scale bar: black bar 0.4 mm, red bar 0.2 mm. D) Concentration of A β 40 and A β 42 in plasma 2 months after treatment. The concentrations of A β 40 and A β 42 in all ELP subgroups were significantly higher than those in PBS subgroups (except the $50 \mu\text{g mL}^{-1}$ i.v. subgroup). Data are presented as mean \pm S.E.M. $*p < 0.05$, $**p < 0.01$, $***p < 0.001$, $****p < 0.0001$ by Student's t test. E) Concentration of A β 40 and A β 42 in RAB fraction of brain homogenate 2 months after treatment. In the i.v. group, significant differences are identified in treatment groups compared with the PBS group. In the i.c.v. group, the concentrations of A β 42 were increased in the $200 \mu\text{g mL}^{-1}$ and $800 \mu\text{g mL}^{-1}$ subgroups. Data are presented as mean \pm S.E.M. $*p < 0.05$, $**p < 0.01$, $***p < 0.001$, $****p < 0.0001$ by Student's t test. F) Western blot of sAPP β and full length (FL) APP of RAB fraction of brain homogenate in i.v. and i.c.v. groups 2 months after treatment. GAPDH acts as the internal control. Black arrows show the target bands. Lane 1: PBS group, lane 2: $50 \mu\text{g mL}^{-1}$ group, lane 3: $200 \mu\text{g mL}^{-1}$ group, lane 4: $800 \mu\text{g mL}^{-1}$ group. FL APP shows no differences among all subgroups. The levels of sAPP β in ELP-treated groups showed a slight upregulation compared to those of PBS control.

21834007, 21801235, and 21907088), the European Union's Horizon 2020 research and innovation programme under the Marie Skłodowska Curie grant agreement No. 713482, National Key R&D Program of China (2018YFA0902600) and the Cure Alzheimer's Fund. We appreciate senior engineer Deli Wang for great guidance about mice experimental technology. We also thank the excellent support from animal experimental platform, core facilities for life science, Jilin University.

Conflict of interest

The authors declare no conflict of interest.

Keywords: Alzheimer's disease · amyloid- β peptides · extracellular elastin · upregulation

How to cite: *Angew. Chem. Int. Ed.* **2019**, *58*, 18703–18709
Angew. Chem. **2019**, *131*, 18876–18882

- [1] S. H. Choi, Y. H. Kim, M. Hebisch, C. Sliwinski, S. Lee, C. D'Avanzo, H. Chen, B. Hooli, C. Asselin, J. Muffat, J. B. Klee, C. Zhang, B. J. Wainger, M. Peitz, D. M. Kovacs, C. J. Woolf, S. L. Wagner, R. E. Tanzi, D. Y. Kim, *Nature* **2014**, *515*, 274–278.
- [2] J. Wang, B. J. Gu, C. L. Masters, Y.-J. Wang, *Nat. Rev. Neurol.* **2017**, *13*, 612–623.
- [3] I. Cherny, E. Gazit, *Angew. Chem. Int. Ed.* **2008**, *47*, 4062–4069; *Angew. Chem.* **2008**, *120*, 4128–4136.
- [4] B. Zott, M. M. Simon, W. Hong, F. Unger, H.-J. Chen-Engerer, M. P. Frosch, B. Sakmann, D. M. Walsh, A. Konnerth, *Science* **2019**, *365*, 559–565.
- [5] A. Spanopoulou, L. Heidrich, H.-R. Chen, C. Frost, D. Hrlle, E. Malideli, K. Hille, A. Grammatikopoulos, J. Bernhagen, M. Zacharias, G. Rammes, A. Kapurniotu, *Angew. Chem. Int. Ed.* **2018**, *57*, 14503–14508; *Angew. Chem.* **2018**, *130*, 14711–14716.
- [6] D. Ellmer, M. Brehms, M. Haj-Yahya, H. A. Lashuel, C. F. W. Becker, *Angew. Chem. Int. Ed.* **2019**, *58*, 1616–1620; *Angew. Chem.* **2019**, *131*, 1630–1634.
- [7] M. T. Heneka, M. J. Carson, J. El Khoury, G. E. Landreth, F. Brosseron, D. L. Feinstein, A. H. Jacobs, T. Wyss-Coray, J. Vitorica, R. M. Ransohoff, K. Herrup, S. A. Frautschy, B. Finsen, G. C. Brown, A. Verkhratsky, K. Yamanaka, J. Koistinaho, E. Latz, A. Halle, G. C. Petzold, T. Town, D. Morgan, M. L. Shinohara, V. H. Perry, C. Holmes, N. G. Bazan, D. J. Brooks, S. Hunot, B. Joseph, N. Deigendesch, O. Garaschuk, E. Boddeke, C. A. Dinarello, J. C. Breitner, G. M. Cole, D. T. Golenbock, M. P. Kummer, *Lancet Neurol.* **2015**, *14*, 388–405.
- [8] F. Huang, J. Wang, A. Qu, L. Shen, J. Liu, J. Liu, Z. Zhang, Y. An, L. Shi, *Angew. Chem. Int. Ed.* **2014**, *53*, 8985–8990; *Angew. Chem.* **2014**, *126*, 9131–9136.
- [9] H. Sun, J. Liu, S. Li, L. Zhou, J. Wang, L. Liu, F. Lv, Q. Gu, B. Hu, Y. Ma, S. Wang, *Angew. Chem. Int. Ed.* **2019**, *58*, 5988; *Angew. Chem.* **2019**, *131*, 6049.
- [10] R. Jakob-Roetne, H. Jacobsen, *Angew. Chem. Int. Ed.* **2009**, *48*, 3030–3059; *Angew. Chem.* **2009**, *121*, 3074–3105.
- [11] M. Gumpelmayer, M. Nguyen, G. Molnár, A. Bousseksou, B. Meunier, A. Robert, *Angew. Chem. Int. Ed.* **2018**, *57*, 14758–14763; *Angew. Chem.* **2018**, *130*, 14974–14979.
- [12] J. K. Mouw, G. Ou, V. M. Weaver, *Nat. Rev. Mol. Cell Biol.* **2014**, *15*, 771–785.
- [13] Y. J. Xie, M. Dougan, N. Jailkhani, J. Ingram, T. Fang, L. Kummer, N. Momin, N. Pishesha, S. Rickelt, R. O. Hynes, H. Ploegh, *Proc. Natl. Acad. Sci. USA* **2019**, *116*, 7624–7631.
- [14] L. W. Lau, R. Cua, M. B. Keough, S. Haylock-Jacobs, V. W. Yong, *Nat. Rev. Neurosci.* **2013**, *14*, 722–729.
- [15] M. Morawski, M. Filippov, A. Tzinia, E. Tsilibary, L. Vargova in *Progress in Brain Research, Vol. 214* (Eds.: A. Dityatev, B. Wehrle-Haller, A. Pitkänen), Elsevier, Amsterdam, **2014**, pp. 207–227.
- [16] S. Soleman, M. A. Filippov, A. Dityatev, J. W. Fawcett, *Neuroscience* **2013**, *253*, 194–213.
- [17] J. Gutierrez, L. Honig, M. S. V. Elkind, J. P. Mohr, J. Goldman, A. J. Dwork, S. Morgello, R. S. Marshall, *Neurology* **2016**, *86*, 1507.
- [18] E. Fonck, G. G. Feigl, J. Fasel, D. Sage, M. Unser, D. A. Rüfenacht, N. Stergiopoulos, *Stroke* **2009**, *40*, 2552–2556.
- [19] N. K. Li, F. G. Quiroz, C. K. Hall, A. Chilkoti, Y. G. Yingling, *Biomacromolecules* **2014**, *15*, 3522–3530.
- [20] S. Arias, F. Freire, M. Calderon, J. Bergueiro, *Angew. Chem. Int. Ed.* **2017**, *56*, 11420–11425; *Angew. Chem.* **2017**, *129*, 11578–11583.
- [21] K. M. Luginbuhl, D. Mozhdehi, M. Dzuricky, P. Yousefpour, F. C. Huang, N. R. Mayne, K. L. Buehne, A. Chilkoti, *Angew. Chem. Int. Ed.* **2017**, *56*, 13979–13984; *Angew. Chem.* **2017**, *129*, 14167–14172.
- [22] M. P. Murphy, H. LeVine 3rd, *J. Alzheimer's Dis.* **2010**, *19*, 311–323.
- [23] O. Hansson, S. Lehmann, M. Otto, H. Zetterberg, P. Lewczuk, *Alzheimer's Res. Ther.* **2019**, *11*, 34.
- [24] W. T. Kimberly, M. J. LaVoie, B. L. Ostaszewski, W. Ye, M. S. Wolfe, D. J. Selkoe, *Proc. Natl. Acad. Sci. USA* **2003**, *100*, 6382–6387.
- [25] P. E. Cramer, J. R. Cirrito, D. W. Wesson, C. Y. Lee, J. C. Karlo, A. E. Zinn, B. T. Casali, J. L. Restivo, W. D. Goebel, M. J. James, K. R. Brunden, D. A. Wilson, G. E. Landreth, *Science* **2012**, *335*, 1503–1506.
- [26] R. M. Deacon, A. Croucher, J. N. Rawlins, *Behav. Brain Res.* **2002**, *132*, 203–213.
- [27] L. Bertram, R. E. Tanzi, *Nat. Rev. Neurosci.* **2008**, *9*, 768–778.
- [28] E. Lauretti, L. Iuliano, D. Praticò, *Ann. Clin. Transl. Neurol.* **2017**, *4*, 564–574.

Manuscript received: September 27, 2019

Accepted manuscript online: October 14, 2019

Version of record online: November 4, 2019